Chaos, Solitons and Fractals 172 (2023) 113507

Contents lists available at ScienceDirect

Chaos, Solitons and Fractals

journal homepage: www.elsevier.com/locate/chaos

Interspecific competition shapes the structural stability of mutualistic networks

Xiangrong Wang [a,*,1], Thomas Peron [b,1], Johan L.A. Dubbeldam [c], Sonia Kéfi [d,e], Yamir Moreno [f,g,h,**]

[a] College of Mechatronics and Control Engineering, Shenzhen University, 518060, Shenzhen, China
[b] Institute of Mathematics and Computer Science, University of São Paulo, 13566-590 São Carlos, SP, Brazil
[c] Faculty of Electrical Engineering, Mathematics and Computer Science, Delft University of Technology, 2600 GA Delft, The Netherlands
[d] ISEM, CNRS, Univ. Montpellier, IRD, EPHE, Montpellier, France
[e] Santa Fe Institute, 1399 Hyde Park Road, Santa Fe, NM 87501, USA
[f] Institute for Biocomputation and Physics of Complex Systems (BIFI), University of Zaragoza, Zaragoza, Spain
[g] Department of Theoretical Physics, Faculty of Sciences, University of Zaragoza, Zaragoza, Spain
[h] CENTAI Institute, Turin, Italy

ARTICLE INFO

Keywords:
Mutualistic networks
Interspecific competition
Structural stability
Species coexistence

ABSTRACT

Mutualistic networks, such as plant–pollinator networks, have attracted increasing attention in the ecological literature in the last decades, not only because of their fascinating natural history, but also because mutualistic interactions have been shown to play a key role in the maintenance of biodiversity. Although inter-specific competition has long been known to be a crucial driver of species coexistence as well, there is a lack of theory investigating the interplay between the structures of competitive and mutualistic networks when jointly considered. Here, we develop an analytical framework to study the structural stability — the range of conditions under which all species coexist stably, *i.e.* where the community is both feasible and stable — of ecological communities in which both mutualistic interactions between plants and pollinators and competitive interactions among plants and among pollinators are present. Using the structure of 50 real networks for mutualistic interactions, combined with analytical and numerical analyses, we show that the structure of the competitive network radically alters the necessary conditions for species coexistence in these communities. Our mathematical framework also allows to accurately characterize the structural stability of these systems. Moreover, we introduce a new metric that accurately links the network structures of competitive and mutualistic interactions to species coexistence. Our results highlight the joint role of the structures of different interaction types to understand the stability of ecological communities and facilitate the analysis of similar natural and artificial systems in which mutualism and competition coexist.

Species rarely live in isolation, but constantly interact with other species with different interaction types, such as predation, competition and mutualism [1]. Mutualism, in which different species interact for their mutual benefit, is ubiquitous in terrestrial ecosystems [2]. Examples include, but are not limited to, plants receiving effective pollination or seed-dispersion by offering rewards in the form of nutrients to their visiting animals, plants gaining resistance to insect herbivores by providing nutrients and shelter to fungi or ants, and leguminous plants obtaining nitrogen by rewarding nitrogen-fixing bacteria.

Inter-specific competition, where species within the same guild compete for shared mutualistic partners, is one of the identified costs when progressing from two species mutualism to species-rich mutualism [3]. This has been reported in field experiments of mutualistic systems of plant and pollinators by Charles Robertson as early as 1895 and was then followed by extensive studies on mutualism e.g. between ants and plants, and between parrots and plants [3–10]. Interspecific competition can limit the biodiversity of plant–pollinator communities by, for example, changing foraging behaviors of pollinators to pollen- or nectar-rich species, while reducing or avoiding the visitation of less-rewarding plants [11–20], and thereby causing an immediate rearrangement of mutualistic interactions [3,21,21,22,22–27].

* Corresponding author.
** Correspondence to: Instituto BIFI, Edificio I+D, Campus Rio Ebro Universidad de Zaragoza, Zaragoza 50018, Spain.
E-mail addresses: xiangrongwang88@gmail.com (X. Wang), yamir@unizar.es (Y. Moreno).
[1] X. Wang and T. Peron contribute equally.

https://doi.org/10.1016/j.chaos.2023.113507
Received 28 March 2023; Accepted 25 April 2023
Available online 16 May 2023

Decades of studies on ecological networks have shown that they have a specific architecture, which plays a key role for their dynamics and stability (e.g. [28–34]). Mutualistic networks — such as plant–pollinator networks for example — have been shown to be highly nested, which has been suggested to contribute to the maintenance of species diversity [30,31]. While competitive interactions have long been considered an important component of mutualistic networks [35–38], they have typically been modeled as an all-to-all connectivity pattern; that is, in a plant–pollinator scenario, all pollinators are considered to compete equally for plants, and all plants are assumed to compete for pollinators regardless of the heterogeneous organization of the mutualistic interactions [36,39]. Competitive interactions in mutualistic networks have also been analyzed using random matrices without considering empirical structures [37,40]. So far, we have however lacked studies explicitly investigating how the joint structure of competitive and mutualistic interactions affects species coexistence.

Studies on random matrices including mixed mutualistic and competitive interactions [37,40] showed opposite stability patterns as those reported in a study of the microbiome network of the human gut, which tunes the proportion of competitive interactions [41]. Furthermore, in networks including both competition and mutualism, each interaction type could play a different role in keeping the system feasible or stable [39,42–45]. These studies suggest that investigating the role of the structure of competitive interactions within mutualistic networks could advance our understanding of the factors that drive the number of species that can stably coexist in communities, one of the oldest questions in ecology [40].

Here, we theoretically investigate the effect of different structures of competitive interactions among plants and among pollinators on the structural stability, *i.e.* the set of conditions (parameters) under which all species are feasible (i.e., have a positive abundance) and are stable to local perturbations, of ecological communities including competitive and mutualistic interactions. Using 50 real networks for the structure of the mutualistic interactions, we develop a framework that accurately predicts the boundary conditions beyond which the communities lose their structural stability. Furthermore, we find that different competitive network structures yield significantly different patterns of structural stability, whose effect can be accurately quantified through a proposed structure predictor. We show that the structure of competitive interactions does have strong implications for the species diversity of ecological communities including both competition and mutualism.

1. Population dynamics of competitive-mutualistic networks

To study the impact of inter-specific competition on communities persistence, we begin by describing a model of the dynamics of plant and pollinator species. We consider a plant–pollinator system consisting of a set $\mathcal{A}$ of N^A pollinator species that interact mutualistically with a set $\mathcal{P}$ of N^P plant species, denoting the total biodiversity by $N = N^P + N^A$. Mutualistic interactions are fully encoded in a $N^P \times N^A$ bipartite matrix K, where $K_{ij} = 1$ if plant species i is pollinated by pollinator species j, and 0 otherwise. Each plant (resp. animal) species is characterized by the abundance s_i^P (resp. s_i^A), whose dynamics depend on the intrinsic growth rate α_i^P (resp. α_i^A) and on the influence of competitive and mutualistic interactions as follows:

$$\begin{cases} \frac{1}{s_i^P}\frac{ds_i^P}{dt} = \alpha_i^P - \beta s_i^P - \beta_0 \sum_{k=1}^{N^P} s_k^P + \frac{\gamma_0 M_i^P}{1+h\gamma_0 M_i^P}, \\ \frac{1}{s_j^A}\frac{ds_j^A}{dt} = \alpha_j^A - \beta s_j^A - \beta_0 \sum_{k=1}^{N^A} \frac{W_{jk}^A}{M_j^A} s_k^A + \frac{\gamma_0 M_j^A}{1+h\gamma_0 M_j^A}, \end{cases} \quad (1)$$

where plant species $i = 1, \ldots, N^P$ and pollinator species $j = 1, \ldots, N^A$. The first term at the right-hand side of the above equations corresponds to the per capita intrinsic growth rate of each species; the second and fourth correspond to the intra-species competition and mutualistic interactions, respectively with β the intensity of intra-specific competition. The intensities of inter-specific competition and mutualism are denoted by β_0 and γ_0, respectively. For plant species i, $M_i^P = \sum_{k\in\mathcal{A}} K_{ik} s_k^A$ is the total abundance of pollinators interacting with plant i. The parameter h, known as the handling time, imposes a nonlinear saturation effect on mutualism.

What distinguishes the dynamics of plant and pollinator species is the definition of the third term, which accounts for the intra-guild inter-specific competition. For plant species, we assume that a mean field competition occurs among all of them with the same strength, irrespective of the mutualistic links each of them has with pollinators. For pollinator species, however, competitive links exist only among pollinator species who share a common plant species, and those interactions are weighted by the relative proportion of the shared plant species [see Fig. 1(c) and Supplementary Fig. S1]. The weight on each competitive link is a collective representation of pollinator individuals competing with each other when they physically land on the exact same plant individual that they both pollinate. Specifically, the weight is set via W_{jk}^A/M_j^A, where $W_{jk}^A = \sum_{p\in\mathcal{P}} K_{jp}^T K_{pk} s_p^P$ represents the total plant abundance shared by pollinators j and k, and $M_j^A = \sum_{p\in\mathcal{P}} K_{jp}^T s_p^P$ represents the total plant abundance interacting with pollinator j. Detailed derivation is provided in the Supplementary Section 1. Notice that inter-specific competition among pollinators in Eq. (1) is asymmetric, since the biomass of shared plant species is normalized by the total biomass of plant species. In other words, two pollinator species i and j perceive each other's competition differently depending on the importance of their shared plants relative to the total abundance of plants with which each pollinator species interact.

Due to the varied competition patterns of pollinator species, we refer to the species dynamics described in Eq. (1) as *the hybrid competition model*. The *full mean field competition model* refers to the scenario in which both plant and pollinator species have a mean field intra-guild competition. The hybrid model is further mapped onto a weighted model numerically explored by Gracia-Lázaro et al. [46], where the plant species also have a weighted competition. In the next section, we present an analytical framework for fixed point solutions of Eq. (1) and analyze the impact of intra-guild competition on species coexistence for networks where the mutualistic structure is based on 50 observed real networks.

2. Structural stability conditions

Our goal here is to present an analytical framework for the structural stability of the nonlinear population dynamics described by Eq. (1). Because of the strong dependence of species coexistence on the specific parameterization, we investigate a range of parameter values in the space spanned by β_0 and γ_0. To investigate the coexistence of structured competition and mutualism, we focus on the parameter space β_0 and γ_0 relevant to species interactions, that is different from previous methods focusing on species intrinsic grow rate [39,47]. Hereafter, we define the "feasible area" as the range of conditions in the (β_0, γ_0)-plane under which the community is structurally stable, that is, an equilibrium point exists that is both feasible and stable. We first derive conditions for a positive equilibrium point, and then further restrict the conditions with local stability.

2.1. Feasibility analysis for the hybrid competition model

The population dynamics of Eq. (1) can be formulated in matrix form to consider all plant and pollinator species: if linear approximations of the nonlinear mutualistic and competitive terms can be derived (see (2), where $A^{P,A}$ encodes the linearly approximated intra-guild inter-specific competitions, while $\widetilde{M}^{P,A}$ encodes the approximated mutualistic interactions. The vectors $s^{P,A}$ contain the abundances of plant and pollinator species, respectively.)

$$\begin{bmatrix} \frac{ds^A}{dt} \\ \frac{ds^A}{dt} \end{bmatrix} = \mathrm{diag}\left(\begin{bmatrix} s^P \\ s^A \end{bmatrix}\right)\left(\begin{bmatrix} \alpha_{\mathrm{eff}}^P \\ \alpha_{\mathrm{eff}}^A \end{bmatrix} - \begin{bmatrix} \beta I + \beta_0 A^P & -\gamma_0 \widetilde{M}^P \\ -\gamma_0 \widetilde{M}^A & \beta I + \beta_0 A^A \end{bmatrix}\begin{bmatrix} s^P \\ s^A \end{bmatrix}\right), \quad (2)$$

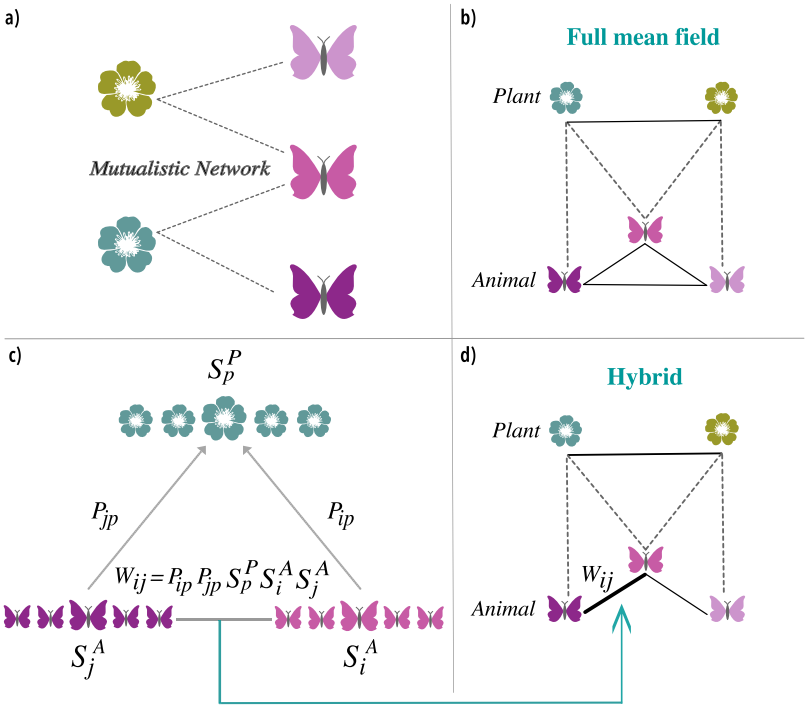

Fig. 1. Inter-specific competition among plant species and among pollinator species. Panel (**a**) shows a minimal mutualistic network that distinguishes the (**b**) full mean-field competition, and the (**d**) hybrid competition scenarios. For the full mean-field competition scenario, competitive interactions are represented by a complete, unweighted graph implying an all to all competition with the same magnitude. For the hybrid competition scenario, intra-guild competition for plant species is represented by a complete, unweighted graph, while for pollinator species the competition is shown by a weighted, structured graph with weights w_{ij} representing the strength of inter-specific competition. The weight is derived from an individual level mechanism in panel (**c**), that considers the probability of two pollinator species landing on the same plant species, see also the Supplementary Section 1.

We start with deriving the intra-guild inter-specific competition matrices $A^{P,A}$. For the hybrid competition model, plant species compete in a mean field fashion and the competition matrix follows $A^P = uu^T - I$, where u is a column vector with all elements 1 and I is the identity matrix. So all entries of A^P are 1, except for the diagonal which is zero. For pollinator species, the inter-specific competition is weighted, and has a nonlinear dependence on the number of species from the other guild. To tackle the nonlinearity and derive the competition matrix A^A, we harness the microscopic perspective of competition among pollinators induced by each plant–pollinator mutualistic interaction. When animal i pollinates plant k (i.e., $K_{ik}^T = 1$), the inter-specific competition between pollinator i and the other pollinators j that also visit plant k reads $\sum_{j\in\mathcal{A}} K_{ik}^T K_{jk}^T s_j^A$. Summing over plants k that are pollinated by animal i and multiplying by the abundance s_k^P yields the total amount of inter-specific competition $\sum_k \left(\sum_{j\in\mathcal{A}} K_{ik}^T K_{jk}^T s_j^A\right) s_k^P$. Armed with the perspective of a single mutualistic interaction, the nonlinear competition term in Eq. (1) can be rewritten as

$$\sum_{j\in\mathcal{A}, j\neq i} \frac{W_{ij}^A}{M_i^A} s_j^A = \frac{\sum_k \left(\sum_{j\in\mathcal{A}, j\neq i} K_{ik}^T K_{jk}^T s_j^A\right) s_k^P}{\sum_k K_{ik}^T s_k^P}. \tag{3}$$

The weighted competition term can be upper and lower bounded by applying the mediant inequality (see Appendix A):

$$\min_{k\in\mathcal{P}} \sum_{\substack{j\in\mathcal{A}\\ j\neq i}} K_{ik}^T K_{jk}^T s_j^A \leq \sum_{\substack{j\in\mathcal{A}\\ j\neq i}} \frac{W_{ij}^A s_j^A}{M_i^A} \leq \max_{k\in\mathcal{P}} \sum_{\substack{j\in\mathcal{A}\\ j\neq i}} K_{ik}^T K_{jk}^T s_j^A. \tag{4}$$

Eq. (4) means that the total amount of competition for pollinator i is bounded by the minimum and maximum competition induced by sharing a single plant species k. Most importantly, Eq. (4) allows disentangling the dependence of pollinator i on plants species and thus enables the embedding of competitive relationships into a competition matrix A^A. The total competitive relations in Eq. (4) can be upper and lower bounded, for pollinator species i, by

$$\min_k K_{ik}^T \left(d_k^P - 1\right) \leq \sum_j A_{ij}^A \leq \max_k K_{ik}^T \left(d_k^P - 1\right), \tag{5}$$

where $d_k^P = \sum_{j\in\mathcal{A}} K_{jk}^T$. Finally, due to the fact that $\max_k K_{ik}^T \left(d_k^P - 1\right) \leq N^P - 1$, (5) indicates that the competition strength of the hybrid model is no stronger than that of the full mean field competition model.

After establishing the bounds for the competition matrix, we now move to derive each element A_{ij}^A for the competition between pollinators i and j. Here, because the weighted competition for pollinator species involves plant species, we need to estimate first the abundance of plants, which in turn depends on pollinators. Through the matrix transformation derived in Eq. (A.4) in Appendix A, we disentangle plant and pollinator species, which allows us to estimate the abundance of plant species. Based on the estimated abundance $\tilde{s_k}^P\left(\beta_0, \gamma_0\right)$ (see Eq. (A.5), the weighted competition for pollinator species i and j is therefore estimated by

$$A_{ij}^A = \frac{\sum_{k\in P} K_{ik}^T K_{jk}^T \tilde{s_k}^P\left(\beta_0, \gamma_0\right)}{\sum_{k\in P} K_{ik}^T \tilde{s_k}^P\left(\beta_0, \gamma_0\right)}. \tag{6}$$

Eq. (6) can be simplified as $A_{ij}^A = \frac{\sum_k K_{ik}^T K_{jk}^T}{d_i^A}$ if assuming homogeneous abundance for plant species. Note that summing up all the competitive pollinators, i.e., $\sum_j A_{ij}^A = \sum_k K_{ik}^T \left(d_k^P - 1\right)/d_i^A$, corresponds to the average competitive degree per mutualistic interaction, in alignment with the lower and upper bounds of the competitive degree derived in Eq. (5). When assuming a mean field competition for both plant and pollinators species (i.e., when the inter-specific competition term of both plant and pollinators is given by $\beta_0 \sum_{j=1}^{N^{P,A}} s_j^{P,A}$), each element of the competitive matrix $A_{ij}^{P,A}$ equals 1 for any $i \neq j, i \in \mathcal{P}$ or $i \in \mathcal{A}$.

We then move to the mutualism and aim at deriving the matrices $\widetilde{M}^{P,A}$. To approximate the nonlinear mutualism, we perform a Taylor

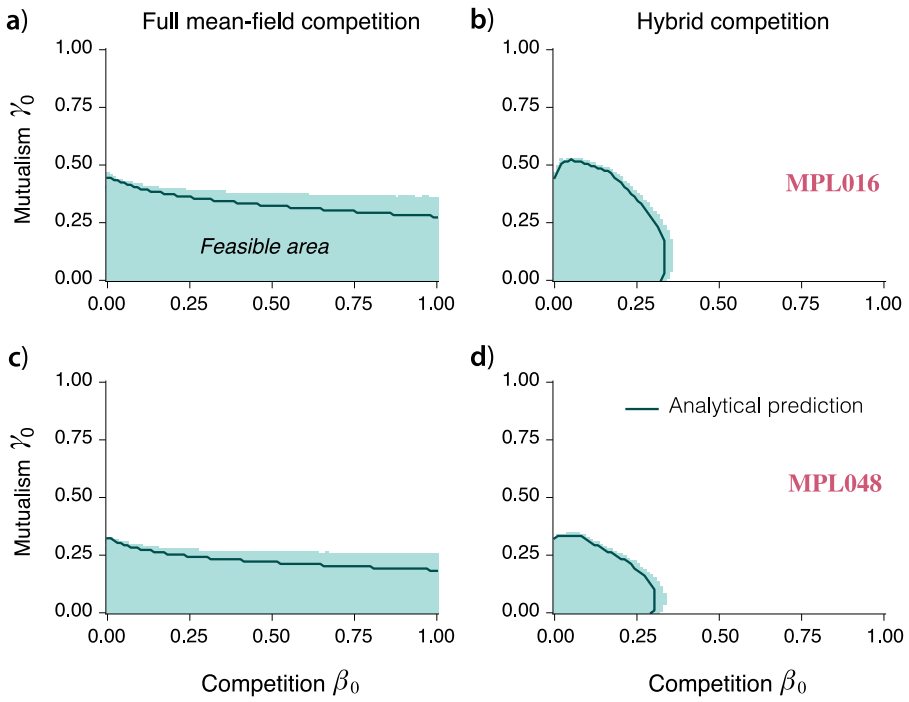

Fig. 2. Inter-specific competition drives the pattern of feasible area. Panels (**a**), (**c**) show the feasible area of the full mean field competition scenario for real world plant–pollinator networks (MPL016, MPL048) from the Web of Life platform [48]. Panels (**b**), (**d**) show the feasible area of the hybrid competition scenario. A point (β_0, γ_0) is colored in light green if all species survive with a positive abundance in the stationary regime of the simulations of Eq. (1) for that parameter choice. Solid lines show the analytical predictions of Eq. (8), where $A^P = A^A = uu^T - I$ for the full mean field competition scenario, and $A^P = uu^T - I$ and A^A given by Eq. (6) for the hybrid competition scenario. Other parameters in simulating the population dynamics are $\alpha_i = 1\ \forall i$, $\beta = 5$, and $h = 0$. The grid size in the parameter space of β_0 and γ_0 is 100×100.

expansion for the mutualistic term in Eq. (1), that is:

$$\frac{(M_0)_i}{1 + h\gamma_0 (M_0)_i} + \left(\frac{M_i}{1 + h\gamma_0 M_i}\right)' \Big|_{M_i=(M_0)_i} (M_i - (M_0)_i). \tag{7}$$

Recall that $M_i^P = \sum_k K_{ik} s_k^A$, encoding the total abundance of pollinators for plant i. Expanding the mutualistic term around a point $(M_0)_i$ close to a fixed point is a difficult task without a prior knowledge of the fixed points of the system, thus the linearization of the dynamics appears to be challenging or even unfeasible. We tackle this problem by analyzing the interplay between the mutualistic interactions and the inter-specific competition, which separately lead to abundance gain and abundance loss at equilibrium. When the mutualistic strength is equal to the competition strength, the species abundance on average follows $\langle s_i \rangle = \frac{\alpha_i}{\beta_i}$. Assuming the average abundance $\langle s_k^A \rangle = \langle s_i \rangle$ for all the animal species pollinating plant i, we linearize the nonlinear population dynamics at $(M_0^P)_i = d_i^P \langle s_i \rangle$ for each plant i, where $d_i^P = \sum_k K_{ik}$ denoting the number of animals pollinating plant i. The fixed point for animal species M_0^A is approximated similarly. The mutualism approximation in Eq. (7) is further bounded by both intra-guild and inter-guild competition, which suppresses the unbounded growth, also known as "an orgy of mutual benefaction" [35] and contributes to stabilize the system.

Combining the competition approximation in Eq. (6) with the mutualism approximation in Eq. (7), the feasible solution for the hybrid competition model is obtained by solving $ds/dt = 0$. Written in a matrix form, a fixed point equilibrium can thus be obtained by solving the linear equation

$$\begin{bmatrix} \alpha_{\text{eff}}^P \\ \alpha_{\text{eff}}^A \end{bmatrix} - \begin{bmatrix} \beta I + \beta_0 A^P & -\gamma_0 \widetilde{M}^P \\ \gamma_0 \widetilde{M}^A & \beta I + \beta_0 A^A \end{bmatrix} \begin{bmatrix} s^P \\ s^A \end{bmatrix} = 0, \tag{8}$$

where $\widetilde{M}^P = -\text{diag}\left(\frac{1}{\left(1+h\gamma_0 \left(M_0^P\right)_i\right)^2}\right) K$, $\widetilde{M}^A = -\text{diag}\left(\frac{1}{\left(1+h\gamma_0 \left(M_0^A\right)_i\right)^2}\right) K^T$ and the vector $\alpha_{\text{eff}}^{P,A} = \alpha^{P,A} + h\left(\frac{\gamma_0 M_0^{P,A}}{1+h\gamma_0 M_0^{P,A}}\right)^2$. Eq. (8) provides an approximate solution for the abundances of real-world mutualistic networks with non-mean field competition.

2.2. Stability analysis of feasible solutions

To ensure that any feasible state is stable, we study their stability by analyzing perturbations around the feasible solution. Let us denote the feasible solution for plant and pollinator species as $(s^*)^{P,A}$. Perturbations around the fixed point $(s^*)^{P,A}$ are governed by the Jacobian matrix, which can be derived as

$$J = \text{diag}\left(\begin{bmatrix} (s^*)^P \\ (s^*)^A \end{bmatrix}\right) \begin{bmatrix} -\beta I - \beta_0 A^P & \gamma_0 \widetilde{M}^P \\ \gamma_0 \widetilde{M}^A & -\beta I - \beta_0 A^A \end{bmatrix}. \tag{9}$$

For fixed point solutions that are positive, i.e., $s_i^* > 0$ for all species i, any feasible solution of the system is stable if all the eigenvalues of the second matrix on the right-hand side have negative real parts. Such a configuration is also called a D-stable state. The stability conditions (negative real parts of the eigenvalues) are translated into the inequality

$$\gamma_0 \leq \max\left(\frac{\beta - \beta_0 \sum_j A_{ij}}{\sum_k \widetilde{M}_{ik}}\right). \tag{10}$$

Until now we have established the approximations for fixed point solutions and conditions for solutions to be stable. In order to theoretically estimate the feasible area, one needs to solve Eq. (8) for different parameters seeking solutions satisfying $s_i^{P,A} > 0$ as well as satisfying negative eigenvalues of the Jacobian matrix. Eq. (8), together with the stability conditions of (9), is applicable to any real and positive value of h, thus enabling the investigation of various mutualistic regimes. The above Eq. (8) is also directly applicable to solve the weighted system in [46].

To evaluate the performance of analytical results, we compare with numerical simulations on real mutualistic networks. Fig. 2 shows the performance of analytical predictions provided by Eq. (8) with direct

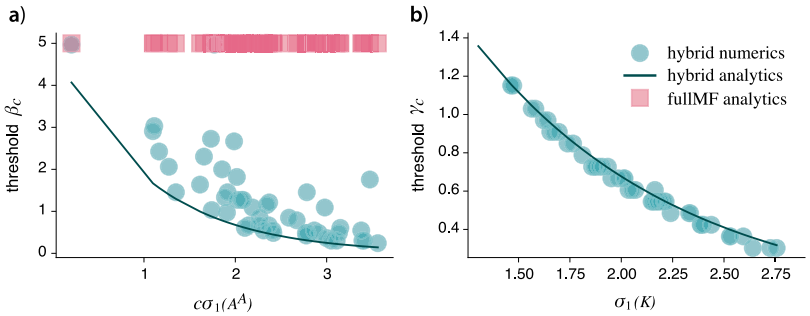

Fig. 3. Thresholds of feasible area and their dependence on network structures. Panel (**a**) shows the dependence of the threshold β_c (which is the critical competition strength before losing any species when setting $\gamma_0 = 0$) on the competitive network structure for the hybrid competition scenario. Circle symbols show the threshold β_c from the numerical results performed on 50 real-world mutualistic networks. The curved line shows the threshold β_c from the analytical prediction of (11). For a mean field competition, the threshold β_c is a constant (shown by the squares), which equals to the intra-specific competition β. Panel (**b**) shows that the threshold γ_c is characterized by the largest singular value of the bipartite network representing all the mutualistic interactions. In the hybrid scenario, the threshold β_c shows a strong dependence on network structure, in contrast, the full mean field scenario shows a threshold that is entirely detached from network structure.

simulations of the dynamical system in Eq. (1) over the parameter space spanned by competition and mutualism strengths, β_0 and γ_0, respectively. For the hybrid competition scenario, the analytical prediction is well confirmed by numerical simulations on real mutualistic networks (Fig. 2b,d). Under mean field competition for plant and pollinator species (i.e., full mean field competition scenario), the feasible area is also well predicted for two real mutualistic networks. In the Supplementary Fig. S2–S5, we show that the approximate solution of Eq. (8) is successful in predicting the feasible area for several real networks in both the full mean-field and hybrid competition scenarios.

Besides checking the validity of our calculations, Fig. 2 also allows us to highlight the marked differences in the dynamics yielded by different competition models. Notice, in particular, how strongly the shape of the feasible area changes from the full mean field to the hybrid weighted competition case: the mere inclusion of heterogeneity in the competition term shifts the region of occurrence of feasible states from strong competition (full mean field) to weak competition (hybrid) with a clear cut-off that is shown later in Eq. (11) to depend on competitive structure. Another noteworthy difference is that full mean field allows decreased mutualism strength with increased competition, while the hybrid allows a nonlinear behavior of mutualistic strength with competition. These results clearly demonstrate how crucial the structure of the inter-specific competition network is for the species coexistence and the diversity of ecological communities.

3. Understanding the network drivers of the structural stability

We now try to understand the network properties that explain the size of the feasible area. We first note that the shape of the feasible area (Fig. 2) is such that, in the hybrid model, there is typically a threshold value of β_0 and γ_0 above which the system is not feasible. Those thresholds are further connected via borderlines that eventually form the feasible area. It turns out that we can derive the expressions of these threshold values and the straight lines connecting them, which can then be used to formulate an approximation of the size of the feasible area — these derived expressions highlight the network properties that drive the feasible area, as we explain next.

We start with a purely competitive system by turning off mutualism ($\gamma_0 = 0$). We then derive the threshold of competition β_c that corresponds to the maximum competition strength that allows a positive equilibrium solution for all species. The threshold β_c can be estimated by the maximum singular value of the competition matrix A^A as

$$\beta_c \approx \frac{\beta}{c\sigma_1\left(A^A\right)}, \tag{11}$$

where $c = \epsilon x_1^T \alpha - x_1^T y_1$, and $\epsilon = \max_i \left(y_1\right)_i / \alpha_i$, which quantifies the distance of angles between x_1 and α and between left and right singular vectors x_1, y_1 belonging to σ_1. A simplified estimation can be obtained by the maximum competitive degree, $\beta_c \geq \frac{\beta}{\max d^A}$, where d^A is the degree vector which corresponds to the row sum vector of the competition matrix A^A. The detailed derivation for the threshold β_c for both plant and pollinator species is provided in Appendix B. In comparison with the full mean competition model, the hybrid competition model exhibits that the threshold value β_c depends on the largest singular value of the competitive matrix.

We next move to a mutualistic system in which the intra-guild competition is turned off ($\beta_0 = 0$). We derive the threshold of mutualistic strength γ_c, above which the pure mutualistic system is not feasible. The threshold γ_c before losing species can be approximated as

$$\gamma_c \leq \frac{\beta}{\sigma_1(K)}, \tag{12}$$

where $\sigma_1(K)$ is the largest singular value of the bipartite matrix K encoding the mutualistic interactions between plants and pollinators. Detailed derivation is shown in Appendix B. Eq. (12) means that this threshold depends on the largest singular value of the plant–pollinator matrix. The performance of the analytical expressions for the thresholds β_c and γ_c is compared to the numerical thresholds that are obtained on 50 real-world mutualistic networks, see Fig. 3. Numerical and analytical results on real networks confirm the dependence of the thresholds on the network properties (Fig. 3).

These two threshold values can now be used to estimate the size of the feasible area if we have an idea of the slope of the line that forms the border of that region. As the feasible area is simultaneously subjected to feasible and stable conditions, we evaluate the structural properties that are relevant to the stability conditions exclusively for feasible equilibrium solutions. The stability condition is translated into stability lines in the parameter space of β_0 and γ_0, as described in Eq. (10). We then calculate the area formed by the thresholds and stability lines. The details of the derivation are presented in Appendix B. This approach leads us to formulate a network predictor for the hybrid competition, denoted as η:

$$\eta_{\text{Hybrid}} = \begin{cases} \beta_c\left(2\gamma_c - r\beta_c\right) & \text{if} \quad \gamma_c \geq r\beta_c, \\ \gamma_c\left(2\beta_c - \gamma_c/r\right) & \text{if} \quad \gamma_c < r\beta_c, \end{cases} \tag{13}$$

where $r = \max_i \left(\frac{\sum_j A^A_{ij}}{\sum_k \widetilde{M}_{ik}}\right)$ denotes the ratio between degrees in the competition matrix A^A and the mutualistic matrix $\widetilde{M}$ (which is reduced to the bipartite matrix K for the case of $h = 0$). The metric η_{Hybrid} correlates surprisingly well with the size of the feasible area, see Fig. 4. Importantly, it depends only on thresholds β_c, γ_c and on the ratio of degrees in the competitive and mutualistic networks. This metric, which naturally emerges from our calculations, suggests that these three properties are the main predictors of the size of the feasible area, namely the species degree in the competitive interactions, the largest singular value of the plant–pollinator network, and the ratio of degrees.

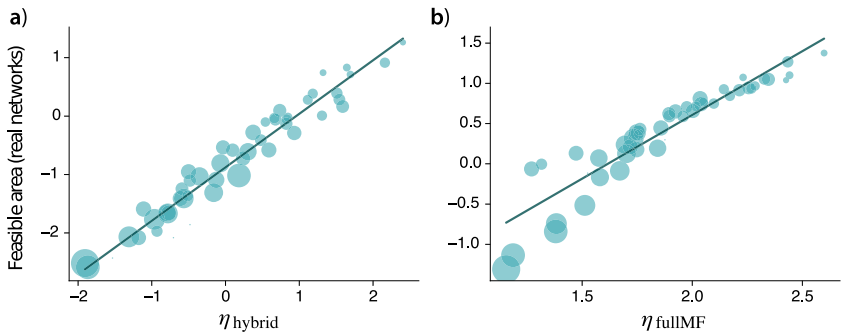

Fig. 4. Feasible area driven by mutualistic and competitive network properties. Panel (**a**) shows, for the hybrid competition scenario, the feasible area of 50 real networks and its relation with the derived network predictor η (Eq. (13)). Panel (**b**) shows the association between feasible area and the derived η (Supplementary Eq. S7) for the full mean field competition scenario. Each circle represents an observed mutualistic network. Solid lines represent regression fits with $R^2 = 0.96$ for the hybrid competition scenario and $R^2 = 0.87$ for the full mean field competition scenario.

We now go one step further and verify if η is a better predictor of the size of the feasible area than other classical metrics of network structure. We select ten of those (see Supplementary Tab. S1 for the metric definitions and calculations) in order to access the impact of both the competitive and mutualistic structure of the corresponding networks. For the competitive network structure, we consider the competition degree and the competition connectance, while for the mutualistic network structure, we consider the mutualistic degree, the mutualistic connectance, the singular values and the nestedness [49]. In addition, we include the ratio between degrees of competition and mutualism, and the total degree of competitive and mutualistic interactions to account for the interplay between competition and mutualism. Using multivariate linear regression for significant predictors, which are identified via dredge [50] from the above ten predictors, the statistical analysis (see Supplementary Figs. S7–S8) suggests that our network predictor η is by far the best predictor of the feasible area for the hybrid competition model.

4. Conclusions

We investigated the extent to which the incorporation of inter-specific intra-guild competition alters the maintenance of biodiversity in mutualistic networks whose structure is based on real data. Compared to a scenario where all species from a guild homogeneously compete with each other, as commonly assumed in the theoretical literature, heterogeneous competition leads to markedly different patterns for the stable coexistence of plant–pollinator networks. Without sufficient empirical data about inter-specific intra-guild competition in plant–pollinator communities, deriving the structure of the competitive links from the observed mutualistic interactions enables us to theoretically explore how the structure of different competition networks affects the structural stability of mutualistic communities.

Our results show that previously identified implications based on homogeneous competition cannot be readily generalized to heterogeneous and structured competition. In particular, we identify here a network predictor of structural stability, which reflects the properties of both the mutualistic and the competitive network, and which performs much better than other properties of mutualistic networks such as nestedness [49]. Therefore, getting information on the structure of competitive networks in mutualistic systems could provide key elements to better understand the forces that constrain the assembly of mutualistic communities during the dynamical coevolutionary processes [51].

More generally, our results contribute to the growing literature investigating how integrating the diversity of interaction types into ecological theory can contribute to improving our understanding of the dynamics and stability of ecological communities [52]. Our results could also have implications for the analysis of similar natural and artificial systems, with economic networks as one of the closest examples.

Declaration of competing interest

The authors declare the following financial interests/personal relationships which may be considered as potential competing interests: Authors (X.W. and Y. M.) serve as the (Associate) Editor of the Journal.

Data availability

Data will be made available on request.

Acknowledgment

X.W. acknowledges the National Natural Science Foundation of China (Grant No. 62003156). T.P. acknowledges FAPESP (Grants No. 2016/23827-6 and No. 2018/15589-3) and PRPI-USP (Grant No. 2022.1.9345.1.2). This research was carried out using the computational resources of the Center for Mathematical Sciences Applied to Industry (CeMEAI) funded by FAPESP (Grant No. 2013/07375-0). S.K. was supported by the grant ANR-18-CE02-0010-01 of the French National Research Agency ANR (project EcoNet). J.L.A.D acknowledges financial support from the European Union's Horizon 2020 research and innovation programme under the Marie Sklodowska-Curie Grant Agreement No. 690817. Y. M. acknowledges partial support from the Government of Aragon and FEDER funds, Spain through grant E36-20R (FENOL), by MCIN/AEI and FEDER funds (grant PID2020-115800GB-I00), and by Soremartec S.A. and Soremartec Italia, Ferrero Group. The funders had no role in the study design, data collection, and analysis, decision to publish, or preparation of the manuscript.

Appendix A. Analytical prediction for the hybrid competition scenario

To accurately predict the population dynamics of the hybrid competition scenario, we approximate the weighted competition and derive the intra-guild competition matrix for plant and pollinator species. In the hybrid competition model of Eq. (1), any pair of plants competes equally, while the competition between two pollinators is assumed to exist if they share plants, and the strength of that competition is proportional to the relative abundance of shared plants. The weighted competition for pollinator species is typically nonlinear due to the dependence on plant species abundances.

To embed the competition relationship in a matrix, the nonlinear weighted competition for pollinators has to be linearly approximated. Let A^A_{ij} denote the weighted competition between pollinator species i and j. If pollinator i shares all its plant species with pollinator j, the weighted term is reduced to a uniformly weighted matrix

$$A^A_{ij} = \begin{cases} 1 & \text{if } \sum_k K^T_{ik} K^T_{jk} = \sum_k K^T_{ik} \\ 0 & \text{otherwise} \end{cases} \tag{A.1}$$

In other words, $A^A_{ij} = 1$ if pollinator species i shares all of its mutualistic interactions with species j, and 0 otherwise. Alternatively, when all plants interacting with pollinator i have uniform abundance values, the weighted competition can be simplified as

$$A^A_{ij} = \frac{d^A_{ij}}{d^A_i}, \tag{A.2}$$

which is the proportion of the shared degree $d^A_{ij} = \sum_k K^T_{ik} K^T_{jk}$ to the mutualistic degree d^A_i of a pollinator i. However, for the observed real-world mutualistic interactions, different plant species typically interact with a distinct set of pollinator species, most likely to cause variations in plant abundance and affect the accuracy of Eq. (A.2).

To obtain the abundance distribution of plant species, we involve a matrix transformation framework to disentangle the dependence of plants on pollinators. Let us rewrite the population dynamics for fixed point solutions as follows

$$\begin{bmatrix} \alpha^P_{\text{eff}} \\ \alpha^A_{\text{eff}} \end{bmatrix} - \begin{bmatrix} \beta I + \beta_0 A^P & -\gamma_0 \widetilde{M}^P \\ -\gamma_0 \widetilde{M}^A & \beta I + \beta_0 A^A \end{bmatrix} \begin{bmatrix} s^P \\ s^A \end{bmatrix} = 0. \tag{A.3}$$

To isolate the dependence of plant species on pollinator species, we perform a Gaussian elimination by multiplying an upper triangular block matrix on the left, which yields

$$\begin{aligned} &\begin{bmatrix} \alpha^P_{\text{eff}} + \gamma_0 \widetilde{M}^P \left(\beta I + \beta_0 A^A\right)^{-1} \alpha^A_{\text{eff}} \\ \alpha^A_{\text{eff}} \end{bmatrix} \\ &= \begin{bmatrix} \left(\beta I + \beta_0 A^P\right) - \gamma_0^2 \widetilde{M}^P \left(\beta I + \beta_0 A^A\right)^{-1} \widetilde{M}^A & 0 \\ -\gamma_0 \widetilde{M}^A & \beta I + \beta_0 A^A \end{bmatrix} \begin{bmatrix} s^P \\ s^A \end{bmatrix}. \end{aligned} \tag{A.4}$$

The plant species s^P can therefore be approximated by

$$\begin{aligned} \tilde{s}^P = &\left(\left(\beta I + \beta_0 A^P\right) - \gamma_0^2 \widetilde{M}^P \left(\beta I + \beta_0 A^A\right)^{-1} \widetilde{M}^A\right)^{-1} \\ &\times \left(\alpha^P_{\text{eff}} + \gamma_0 \widetilde{M}^P \left(\beta I + \beta_0 A^A\right)^{-1} \alpha^A_{\text{eff}}\right) \end{aligned} \tag{A.5}$$

where the approximated mutualistic matrix $\widetilde{M}^{A,P}$ is obtained via Eq. (7). For the hybrid model, the competition for plants is assumed to have a mean field competition, that is $A^P = uu^T - I$ where u is the all one column vector and uu^T encodes the all one matrix. The competition between plant species k and p can be equivalently written as

$$A^P_{kp} = 1 - \delta_{kp} \tag{A.6}$$

and the competition matrix A^A for pollinators is approximated by Eq. (A.2). Once the abundance of plant species is approximated, the weighted competition for pollinator species i and j can be expressed as

$$A^A_{ij} = \frac{\sum_{k\in P} K^T_{ik} K^T_{jk} \tilde{s_k}^P}{\sum_{k\in P} K^T_{ik} \tilde{s_k}^P}. \tag{A.7}$$

Finally, with the approximated competitive matrices $A^{P,A}$ and mutualistic matrices $\widetilde{M}^{A,P}$, the fixed point solution can be obtained by Eq. (A.3).

To further ensure that any feasible solutions are stable to small perturbations, we provide the detailed stability analysis for small perturbations around the equilibrium point. A small perturbation around a fixed point s^* can be denoted as $\delta_s = s - s^*$. The change of perturbation with time is $d\delta_s/dt = J\delta_s$. To determine the stability of the equilibrium point, we analyze the Jacobian matrix J, which is written as

$$J = -\text{diag}\left(s^*\right)\left(\beta I - B\right). \tag{A.8}$$

where B is expressed in the form of a block matrix as

$$B = \begin{bmatrix} -\beta_0 A^P & \gamma_0 \widetilde{M}^P \\ \gamma_0 \widetilde{M}^A & -\beta_0 A^A \end{bmatrix}. \tag{A.9}$$

The decay of the perturbation requires all eigenvalues of the Jacobian matrix to be negative. For positive solutions, $s^*_i > 0$ for any i, the stability condition requires all eigenvalues of $\beta I - B$ to be positive. In other words, all eigenvalues of B are smaller than β, which is translated into

$$\lambda_i(B) \le \beta_0 \sum_j A_{ij} + \gamma_0 \sum_k \widetilde{M}_{ik} \le \beta, \tag{A.10}$$

where A is the intra-guild interspecific competition matrix, and $\widetilde{M}$ encodes the linearly approximated mutualism term. Hence, the stability condition is

$$\gamma_0 \le \max\left(\frac{\beta - \beta_0 \sum_j A_{ij}}{\sum_k \widetilde{M}_{ik}}\right). \tag{A.11}$$

Eq. (A.11) implies that the mutualistic strength γ_0 decreases with the competitive strength β_0, and its slope depends on the ratio between the competitive and mutualistic degrees. When a mutualistic structure is fixed (where the threshold γ_c is fixed), the larger the absolute slope of the stability line, i.e. the ratio of competitive degree to mutualistic degree [Eq. (A.11)], the smaller the range of parameters that allows species to coexist.

Supplementary Figures S2 and S3 show simulation results with analytical predictions for more real plant–pollinator networks. As it can be seen, for $h = 0$ (Fig. S2), the matching between the numerical results and our calculations is remarkable. Notice, in particular, how the detailed contour of the feasible area in the hybrid competition scenario is almost exactly captured by the analytical curves. For the case of $h = 0.1$ in Fig. S3 the analytical results accurately predict the feasible area for a large range of mutualistic strength γ_0, with exceptions at a high value of mutualism due to the saturation effect. All in all, our analytical results work very well for a variety of real mutualistic networks.

Appendix B. Derivation of the network property η

In this section, we derive a network property, η, that is shown to be a predictor of the feasible area. We start by deriving the threshold values of competitive and mutualistic strength below which the fixed point solutions are positive. Specifically, the threshold β_c corresponds to the maximum allowed β_0 that results in feasible solutions in a purely competitive system ($\gamma_0 = 0$), while the threshold γ_c is analogously defined for a mutualistic system with inter-specific competition being turned off ($\beta_0 = 0$). These thresholds, as we shall derive, highlight network properties that drive feasible area.

We first analyze the threshold β_c on a purely competitive system by turning off the mutualistic interactions ($\gamma_0 = 0$). For the purely competitive system, species abundance s^* at equilibrium can be obtained by

$$\alpha^{A,P}_{\text{eff}} - \left(\beta I + \beta_0 A^{A,P}\right) s^* = 0. \tag{B.1}$$

Because plant species have a different competition pattern from the pollinator species in the hybrid model, we derive fixed point solutions for plants and pollinators separately. To solve the equilibrium abundance for plant species, we decompose the competition matrix as $A^P = \sum_{k=1}^{N^P} \lambda_k u_k u_k^T$. The competition matrix under the mean field assumption has the form $A^P = uu^T - I$, where uu^T represents the all one matrix and I is the identity matrix. The feasibility of the solution for plants is guaranteed, for any nonnegative value of β_0, which reads

$$s^* = \sum_k \frac{1}{\beta + \beta_0 \lambda_k} u_k u_k^T \alpha^P_{\text{eff}} = \frac{\alpha^P_{\text{eff}}}{\beta + \beta_0 (N-1)} \ge 0.$$

In addition, when the competition strength satisfies $\beta_0 \le \beta$, the above fixed point solution is stable against small perturbations, due to the fact that all eigenvalues of the corresponding Jacobian matrix are nonpositive, which are $\lambda_1 = -\left(\beta + \beta_0 (N-1)\right) < 0$ and $\lambda_k = \beta_0 - \beta \le 0$, for $k = 2, \ldots, N^P$. Combining the constrains of both positive equilibrium and stability, the threshold β_c for plant species of mean field competition reads

$$\beta_c = \beta \qquad \text{(mean field competition)}. \tag{B.2}$$

We now move to deriving the threshold β_c for pollinator species, which are assumed to have a weighted competition among those who share plants. For a purely competitive system, the inter-specific competition matrix for pollinator species has the following form

$$A^A = \mathrm{diag}\left(1/K^T u\right) K^T K - I, \tag{B.3}$$

where u is the all one vector with size being the number of pollinator species. Substituting the above described competition matrix into the governing Eq. (B.1) of population dynamics yields the fixed point abundance for pollinator species, which follows $s^* = \left(\beta I + \beta_0 A^A\right)^{-1} \alpha^A$. By further imposing the feasible condition that $s_i^* > 0$ for all pollinator species i, the corresponding threshold β_c can be obtained by evaluating the solution until negative solution appears. The agreement with numerically obtained thresholds for 50 real mutualistic networks is shown in Supplementary Fig. S6. In case of non-invertible competition matrix, the problem can be mapped into the phase I of simplex methods for linear programming [53].

Here, in order to understand the structural determinants of the threshold β_c, we derive an analytical estimation associating the threshold β_c with network structural properties. We decompose the intra-guild competition matrix A^A as $A^A = \sum_{k=1}^{N^A} \sigma_k y_k x_k^T$, where σ_k is the singular value, and the column vectors y_k and x_k are the corresponding left and right singular vectors. Because the competition matrix for pollinator species is asymmetric for most observed mutualistic networks, we choose the singular value decomposition. By applying the Sherman–Morrison formula, we obtain the following approximation for the inverse of the competition matrix:

$$\left(\beta I + \beta_0 A^A\right)^{-1} \approx \frac{1}{\beta}\left(I - \frac{\beta_0 \sigma_1 y_1 x_1^T}{\beta + \beta_0 \sigma_1 x_1^T y_1}\right). \tag{B.4}$$

By further imposing the condition that $s_i^* > 0$ for any species i, we derive the following approximation for the threshold β_c:

$$\beta_c \approx \frac{\beta}{c\sigma_1(A^A)}, \tag{B.5}$$

where $\sigma_1(A^A)$ is the largest singular value and $c = x_1^T \alpha \max(y_1)_i/\alpha_i - x_1^T y_1$, in which y_1 and x_1 are the corresponding left and right singular vectors belonging to σ_1, respectively. In addition, one can further loose the approximation by applying the inequality [54]

$$\alpha \geq \sum_{j\neq i, j=1}^{N^A} \left(\frac{\alpha\beta_0}{\beta}\right) A_{ij}^A, \tag{B.6}$$

which yields an estimation for the threshold β_c as

$$\beta_c \approx \frac{\beta}{\max d^A}, \tag{B.7}$$

where $d^A = A^A u$ is the degree of the intra-guild competitive matrix derived in Eq. (B.3). Moreover, the value d_i^A for pollinator i follows $d_i^A = \sum_{k\neq i} K_{ik}^T (Ku)_k/(Ku)_i$, which is the average inter-specific competition introduced by a single mutualistic interaction. The approximations of both Eq. (B.5) and (B.7) indicate that the threshold β_c significantly depends on the competitive structure.

We next derive the threshold for the mutualistic strength γ_0 when turning off the inter-specific competition. For the mutualistic system with $\beta_0 = 0$, the species abundance at equilibrium satisfies the following equation

$$\alpha - \left(\beta I - \gamma_0 \widetilde{M}\right) s^P = 0. \tag{B.8}$$

If the interaction matrix $\beta I - \gamma_0 \widetilde{M}$ is a M-matrix, in other words, $\widetilde{M}$ is a elementary-wise positive matrix and $\beta > \gamma_0 \lambda_1(\widetilde{M})$, then the solution to the linear system Eq. (B.8) is positive for each species. For a mutualistic system of plant and pollinator species, the matrix $\widetilde{M}$ has the following block structure

$$\widetilde{M} = \begin{bmatrix} & K \\ K^T & \end{bmatrix}, \tag{B.9}$$

where the largest eigenvalue of $\widetilde{M}$ is equivalent to the largest singular value $\sigma_1(K)$ of the bipartite matrix K of plant and pollinator interactions. Hence, the threshold γ_c for mutualistic interactions before losing any species is given by

$$\gamma_c \approx \frac{\beta}{\sigma_1(K)}. \tag{B.10}$$

Supplementary Figure S6 shows the agreement between numerical thresholds on 50 real mutualistic networks and the theoretical predictions of Eq. (B.10).

As the feasible area is simultaneously subjected to feasible and stable conditions, which might not necessarily coincide, we evaluate the structural properties that are relevant to the stability conditions exclusively for feasible equilibrium solutions. By analyzing the Jacobian matrix obtained in Eq. (9), a feasible solution is stable if all eigenvalues of the Jacobian matrix are negative. The stability condition is translated into the stability line in the parameter space of β_0 and γ_0 described by Eq. (10). Finally, by combining the stability line and the thresholds β_c and γ_c, we formulate the network property η_{Hybrid} for the hybrid competition scenario, from which we establish Eq. (13).

The formulated network property η consists of thresholds and boundary lines that are determined by competitive and mutualistic structures. In other words, the network property η, as an integrated network structure, quantifies the joint effect of competitive and mutualistic structures on the shape of the feasible area.

Appendix C. Supplementary data

Supplementary material related to this article can be found online at https://doi.org/10.1016/j.chaos.2023.113507.

References

[1] Townsend CR, Begon M, Harper JL, et al. Essentials of ecology. 2nd ed.. Blackwell Science; 2003.

[2] Bascompte J, Jordano P. Mutualistic networks, Vol. 70. Princeton University Press; 2013.

[3] Palmer TM, Stanton ML, Young TP. Competition and coexistence: Exploring mechanisms that restrict and maintain diversity within mutualist guilds. Amer Nat 2003;162(S4):S63–79.

[4] Connell JH. On the prevalence and relative importance of interspecific competition: Evidence from field experiments. Amer Nat 1983;122(5):661–96.

[5] Campbell DR, Motten AF. The mechanism of competition for pollination between two forest herbs. Ecology 1985;66(2):554–63.

[6] Feinsinger P. Effects of plant species on each other's pollination: Is community structure influenced? Trends Ecol Evol 1987;2(5):123–6.

[7] Davidson DW, Morton SR. Competition for dispersal in ant-dispersed plants. Science 1981;213(4513):1259–61.

[8] Stanton ML. Interacting guilds: Moving beyond the pairwise perspective on mutualisms. Amer Nat 2003;162(S4):S10–23.

[9] Blanco G, Hiraldo F, Rojas A, Dénes FV, Tella JL. Parrots as key multilinkers in ecosystem structure and functioning. Ecol Evol 2015;5(18):4141–60.

[10] Montesinos-Navarro A, Hiraldo F, Tella JL, Blanco G. Network structure embracing mutualism–antagonism continuums increases community robustness. Nat Ecol Evol 2017;1(11):1661.

[11] Chittka L, Schürkens S. Successful invasion of a floral market. Nature 2001;411(6838):653.

[12] Brown BJ, Mitchell RJ, Graham SA. Competition for pollination between an invasive species (purple loosestrife) and a native congener. Ecology 2002;83(8):2328–36.

[13] Mitchell RJ, Flanagan RJ, Brown BJ, Waser NM, Karron JD. New frontiers in competition for pollination. Ann Botany 2009;103(9):1403–13.

[14] Aschehoug ET, Brooker R, Atwater DZ, Maron JL, Callaway RM. The mechanisms and consequences of interspecific competition among plants. Annu Rev Ecol Evol Syst 2016;47:263–81.

[15] Wagg C, Jansa J, Stadler M, Schmid B, Van Der Heijden MGA. Mycorrhizal fungal identity and diversity relaxes plant–plant competition. Ecology 2011;92(6):1303–13.

[16] Ghazoul J. Floral diversity and the facilitation of pollination. J Ecol 2006;94(2):295–304.

[17] Fricke EC, Tewksbury JJ, Wandrag EM, Rogers HS. Mutualistic strategies minimize coextinction in plant–disperser networks. Proc R Soc B 2017;284(1854):20162302.

[18] Valdovinos FS, Moisset de Espanés P, Flores JD, Ramos-Jiliberto R. Adaptive foraging allows the maintenance of biodiversity of pollination networks. Oikos 2013;122(6):907–17.
[19] Valdovinos FS, Brosi BJ, Briggs HM, Moisset de Espanés P, Ramos-Jiliberto R, Martinez ND. Niche partitioning due to adaptive foraging reverses effects of nestedness and connectance on pollination network stability. Ecol Lett 2016;19(10):1277–86.
[20] Valdovinos FS, Berlow EL, Moisset de Espanés P, Ramos-Jiliberto R, Vázquez DP, Martinez ND. Species traits and network structure predict the success and impacts of pollinator invasions. Nature Commun 2018;9(1):1–8.
[21] Graham CH, Parra JL, Rahbek C, McGuire JA. Phylogenetic structure in tropical hummingbird communities. Proc Natl Acad Sci 2009;106(Supplement 2):19673–8.
[22] Brown JH, Bowers MA. Community organization in hummingbirds: Relationships between morphology and ecology. The Auk 1985;102(2):251–69.
[23] Wilmer P. Pollination and floral ecology. Princeton University Press; 2011.
[24] Johnson LK, Hubbell SP. Aggression and competition among stingless bees: Field studies. Ecology 1974;55(1):120–7.
[25] Roubik DW. Foraging behavior of competing africanized honeybees and stingless bees. Ecology 1980;61(4):836–45.
[26] Roubik DW, Moreno JE, Vergara C, Wittmann D. Sporadic food competition with the African honey bee: Projected impact on neotropical social bees. J Trop Ecol 1986;2(2):97–111.
[27] Ramos-Jiliberto R, Valdovinos FS, Moisset de Espanés P, Flores JD. Topological plasticity increases robustness of mutualistic networks. J Anim Ecol 2012;81(4):896–904.
[28] de Ruiter PC, Neutel A-M, Moore JC. Energetics, patterns of interaction strengths, and stability in real ecosystems. Science 1995;269(5228):1257–60.
[29] Neutel A-M, Heesterbeek JA, de Ruiter PC. Stability in real food webs: Weak links in long loops. Science 2002;296(5570):1120–3.
[30] Bascompte J, Jordano P, Melián CJ, Olesen JM. The nested assembly of plant–animal mutualistic networks. Proc Natl Acad Sci 2003;100(16):9383–7.
[31] Thébault E, Fontaine C. Stability of ecological communities and the architecture of mutualistic and trophic networks. Science 2010;329(5993):853–6.
[32] Stouffer DB, Bascompte J. Compartmentalization increases food-web persistence. Proc Natl Acad Sci 2011;108(9):3648–52.
[33] Kéfi S, Berlow EL, Wieters EA, Joppa LN, Wood SA, Brose U, et al. Network structure beyond food webs: Mapping non-trophic and trophic interactions on Chilean rocky shores. Ecology 2015;96(1):291–303.
[34] Kéfi S, Miele V, Wieters EA, Navarrete SA, Berlow EL. How structured is the entangled bank? The surprisingly simple organization of multiplex ecological networks leads to increased persistence and resilience. PLOS Biol 2016;14(8):1–21.
[35] May RM. Models for two interacting populations. Theor Ecol: Principles Appl 1976;49–70.
[36] Bastolla U, Fortuna MA, Pascual-Garcia A, Ferrera A, Luque B, Bascompte J. The architecture of mutualistic networks minimizes competition and increases biodiversity. Nature 2009;458(7241):1018.
[37] Allesina S, Tang S. Stability criteria for complex ecosystems. Nature 2012;483(7388):205.
[38] Suweis S, Simini F, Banavar JR, Maritan A. Emergence of structural and dynamical properties of ecological mutualistic networks. Nature 2013;500(7463):449.
[39] Rohr RP, Saavedra S, Bascompte J. On the structural stability of mutualistic systems. Science 2014;345(6195):1253497.
[40] May RM. Will a large complex system be stable? Nature 1972;238(5364):413.
[41] Coyte KZ, Schluter J, Foster KR. The ecology of the microbiome: Networks, competition, and stability. Science 2015;350(6261):663–6.
[42] Pascual-García A, Bastolla U. Mutualism supports biodiversity when the direct competition is weak. Nature Commun 2017;8(1):1–13.
[43] Saavedra S, Rohr RP, Olesen JM, Bascompte J. Nested species interactions promote feasibility over stability during the assembly of a pollinator community. Ecol Evol 2016;6(4):997–1007.
[44] Saavedra S, Rohr RP, Bascompte J, Godoy O, Kraft NJB, Levine JM. A structural approach for understanding multispecies coexistence. Ecol Monograph 2017;87(3):470–86.
[45] Ohlmann M, Munoz F, Massol F, Thuiller W. Assessing mutualistic metacommunity capacity by integrating spatial and interaction networks. 2022, arXiv preprint arXiv:2206.11029.
[46] Gracia-Lázaro C, Hernández L, Borge-Holthoefer J, Moreno Y. The joint influence of competition and mutualism on the biodiversity of mutualistic ecosystems. Sci Rep 2018;8(1):1–9.
[47] Grilli J, Adorisio M, Suweis S, Barabás G, Banavar JR, Allesina S, et al. Feasibility and coexistence of large ecological communities. Nature Commun 2017;8(1):1–8.
[48] http://www.web-of-life.es/. Accessed 28 March 2023.
[49] Mariani MS, Ren Z-M, Bascompte J, Tessone CJ. Nestedness in complex networks: Observation, emergence, and implications. Phys Rep 2019;813:1–90.
[50] Barton K, Barton MK. Package 'Mumin'. Version 2015;1(18):439.
[51] Guimarães Jr PR, Pires MM, Jordano P, Bascompte J, Thompson JN. Indirect effects drive coevolution in mutualistic networks. Nature 2017;550(7677):511.
[52] Kéfi S, Berlow EL, Wieters EA, Navarrete SA, Petchey OL, Wood SA, et al. More than a meal ... integrating non-feeding interactions into food webs. Ecol Lett 2012;15(4):291–300.
[53] Dantzig GB. Origins of the simplex method. In: A history of scientific computing. 1990, p. 141–51.
[54] Kaykobad M. Positive solutions of positive linear systems. Linear Algebra Appl 1985;64:133–40.